

*Supporting Information for*

## **Naphthalene Diimide-Incorporated Helical Thienoacene: A Helical Molecule with High Electron Mobility, Good Solubility, and Thermally Stable Solid Phase**

<sup>a</sup>Department of Chemistry, Graduate School of Science and Engineering, Saitama University, Shimo-okubo, Sakura-ku, Saitama, 338-8570, Japan.

<sup>b</sup>Graduate School of Natural Science and Technology, Kanazawa University, Kakuma-machi, Kanazawa 920-1192, Japan.

<sup>c</sup>Institute for Frontier Science Initiative (InFiniti), Kanazawa University, Kakuma-machi, Kanazawa, Ishikawa 920-1192, Japan.

<sup>d</sup>Nanomaterial Research Institute (NanoMaRI), Kanazawa University, Kakuma-machi, Kanazawa, Ishikawa 920-1192, Japan.

<sup>e</sup>Department of Chemistry, College of Science, Rikkyo University, 3-34-1 Nishi-Ikebukuro, Toshima-ku, Tokyo 171-8501, Japan

### Contents

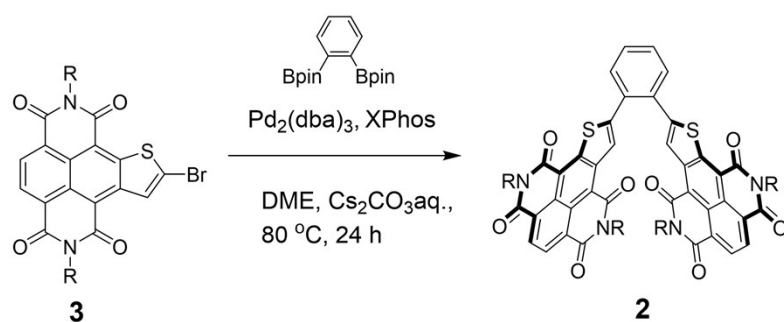
1. Experimental
2. Comparison of phase transition temperature and solubility  
between linear and helically-twisted polycyclics
3. DFT calculation results
4. Dihedral angles of the inner C-C bonds and bonds of NDI moiety of **1**
5. Single-crystal X-Ray measurement
6. Changes of XRD patterns and AFM images of thin film of **1** upon thermal annealing
7. Fabrication methods and properties of OTFT devices
8. NMR charts
9. References

## 1. Experimental

### 1-1. Synthesis

#### General

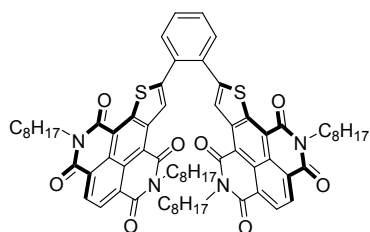
All chemicals and solvents are of reagent grade unless otherwise indicated. Compound **2** was synthesized according to the reported procedures.<sup>1</sup> Photoreaction was carried out using a 450 W high-pressure mercury lamp (Ushio UM-452). Nuclear magnetic resonance (NMR) spectra were recorded on JEOL-ECS400 in deuterated chloroform (CDCl<sub>3</sub>) solution with tetramethylsilane as internal standard; chemical shifts ( $\delta$ ) are reported in parts per million. Melting points were detected on a BUCHI M565 instrument. IR spectra were recorded on a Shimadzu IRPrestige-21 FT-IR spectrophotometer using a KBr pellet.



(R = C<sub>8</sub>H<sub>17</sub>)

**Scheme S1.** Synthesis of compound **2**.

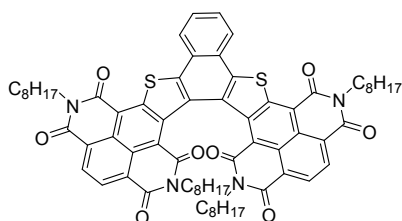
#### **1,2-Bis(naphtho[2,3-*b*]thiophen-2-yl)benzen-*N,N',N'',N'''*-tetraoctyl-4,4',5,5',8,8',9,9'-octacarboxytetramide (2)**



Compound **3** (50 mg, 0.080 mmol), cesium carbonate (560 mg, 1.6 mmol), tris(dibenzylideneacetone)dipalladium(0) (15 mg, 1.6  $\mu$ mol), XPhos (33 mg, 6.4 mmol) and 1,2-benzenediboronic acid bis(pinacol) ester (130 mg, 0.40 mmol) were added to a 20 mL vial equipped

with a magnetic stir bar. The vial was evacuated and backfilled with Ar (this process was repeated three times). Degassed 1,2-dimethoxyethane (40 mL) and water (500  $\mu$ L) was added to the vial under Ar atmosphere. The reaction mixture was stirred at 80°C for 24 h and cooled to room temperature. The reaction mixture was loaded onto a silica-gel column, and compound **2** was isolated by silica-gel column chromatography (eluent: CH<sub>2</sub>Cl<sub>2</sub>/hexane = 1/2). After further purification by reprecipitation, compound **2** was obtained as red solid (200 mg, 44%). <sup>1</sup>H NMR (400 MHz, CDCl<sub>3</sub>):  $\delta$  = 8.99 (s, 2H, Ar-*H*), 8.76 (d, *J* = 7.56 Hz, 2H, Ar-*H*), 8.74 (d, *J* = 7.56, 2H, Ar-*H*), 7.90–7.84 (m, 2H, Ar-*H*), 7.70–7.64 (m, 2H, Ar-*H*), 4.16–4.06 (m, 8H, CH<sub>2</sub>), 1.74–1.58 (m, 8H, CH<sub>2</sub>), 1.42–1.15 (m, 40H, CH<sub>2</sub>), 0.91–0.80(m, 12H, CH<sub>3</sub>) ppm; <sup>13</sup>C NMR (100 MHz, CDCl<sub>3</sub>):  $\delta$  = 163.1, 163.0, 162.7, 162.6, 156.2, 146.2, 143.5, 133.1, 131.7, 130.2 (two carbons), 130.1, 126.4, 125.5, 124.9, 124.4, 123.5, 118.3, 118.3, 41.0, 40.9, 31.8, 31.7, 29.3, 29.2, 29.2, 29.2, 28.0 (two carbons), 27.1, 27.1, 22.6, 22.6, 14.1, 14.1 ppm; Mp: 227–228 °C (decompose, under air); IR(KBr)  $\nu$  = 1698, 1656 cm<sup>-1</sup> (C=O); HRMS (APCI) *m/z* calcd for C<sub>70</sub>H<sub>79</sub>N<sub>4</sub>O<sub>8</sub>S<sub>2</sub> [M+H]<sup>+</sup> 1167.5339, found 1167.5336.

**Naphtho[1,2-*b*:3,4-*b'*]bis(*N,N'*-dioctylnaphtho[2,3-*b*]thiophene-4,5,8,9-tetracarboxydiimide) (1)**



Compound **2** (97 mg, 0.085 mmol), iodine (111 mg, 0.44 mmol), benzene (300 mL) were added to a standard photochemical reactor equipped with a magnetic stir bar. The reaction mixture was bubbled for 1 h with nitrogen and illuminated by a mercury lamp for 2 h under nitrogen atmosphere while stirring in an immersion well. After the solvent was removed under reduced pressure, the residue was diluted with dichloromethane, washed with sodium thiosulfate solution and water, dried over sodium sulfate, and evaporated to dryness. The crude product was loaded onto a silica-gel column, and compound **1** was isolated by silica-gel column chromatography (eluent: CH<sub>2</sub>Cl<sub>2</sub>/hexane = 1/2). After further purification by reprecipitation, compound **1** was obtained as a dark-green solid (86 mg, 88%). <sup>1</sup>H NMR (CDCl<sub>3</sub>, 400 MHz):  $\delta$  = 8.87 (d, *J* = 7.56 Hz, 2H, Ar-*H*), 8.83 (d, *J* = 7.56, 2H, Ar-*H*),

8.53–8.46 (m, 2H, Ar-*H*), 7.94–7.87 (m, 2H, Ar-*H*), 4.43–4.30 (m, 4H, *CH*<sub>2</sub>), 3.25–3.12 (m, 2H, *CH*<sub>2</sub>), 2.25–2.11 (m, 2H, *CH*<sub>2</sub>), 1.96–1.82 (m, 4H, *CH*<sub>2</sub>), 1.60–1.49 (m, 2H, *CH*<sub>2</sub>), 1.49–1.25 (m, 16H, *CH*<sub>2</sub>), 1.21–0.69 (m, 36H) ppm; <sup>13</sup>C NMR (100 MHz, CDCl<sub>3</sub>): δ = 163.6, 162.7, 162.5, 162.1, 145.1, 143.7, 141.5, 130.4, 130.4, 130.2, 129.0, 127.5, 126.5, 126.4, 125.4, 124.7, 124.0, 119.3, 118.2, 41.4, 40.9, 31.8, 31.6, 29.4, 29.3, 28.9, 28.9, 28.2, 27.2, 27.0, 26.5, 22.7, 22.5, 14.1, 14.0 ppm; Mp: >300 °C. IR(KBr) ν = 1699, 1654 cm<sup>-1</sup> (C=O); HRMS (APCI) *m/z* calcd for C<sub>70</sub>H<sub>77</sub>N<sub>4</sub>O<sub>8</sub>S<sub>2</sub> [M+H]<sup>+</sup> 1165.5183, found 1165.5186.

## 1-2. Physicochemical studies

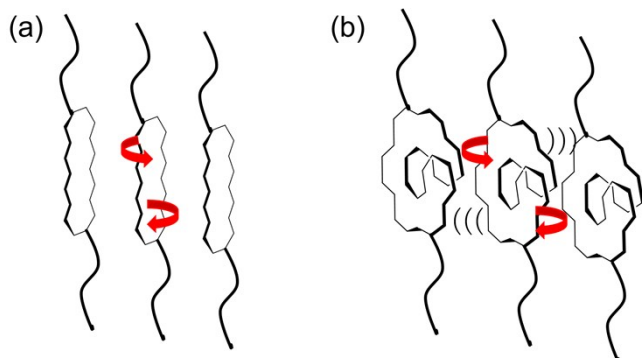
UV-vis absorption spectra were measured on a Shimadzu UV-3600 spectrometer in chloroform solution (concentration: ca. 10<sup>-5</sup>M). Cyclic voltammograms (CVs) were recorded on an ALS Electrochemical Analyzer Model 612D in benzonitrile containing tetrabutylammonium hexafluorophosphate (Bu<sub>4</sub>NPF<sub>6</sub>, 0.1 M) as supporting electrolyte at a scan rate of 100 mV s<sup>-1</sup>. Counter and working electrodes were made of Pt. All the potentials were calibrated with the standard ferrocene/ferrocenium redox couple (Fc/Fc<sup>+</sup>: *E*<sub>1/2</sub> = +0.47 V). Differential scanning calorimetry (DSC) was carried out under nitrogen on a SII DSC 7020 at a scanning rate of 10 °C min<sup>-1</sup>. AFM images were obtained on a Nanotechnology, Inc. scanning probe microscope Nanocute system. X-ray diffractions of thin films deposited on the Si/SiO<sub>2</sub> substrate were obtained with X-ray diffractometry (Rigaku diffractometer, Tokyo, Japan) with a Cu Kα source (λ = 1.541 Å) in the air.

## 1.3. Theoretical calculations

Geometry optimizations and normal mode calculations of isolated molecules were performed at the B3LYP/6-31G\* level using the Gaussian 09 program package.<sup>2</sup> The isomerization energy of **1** was calculated by using Reaction Plus Pro (HPC System Inc.).<sup>3</sup> All the model compounds have methyl groups at their imide moieties to simplify the calculations.

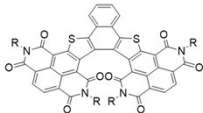
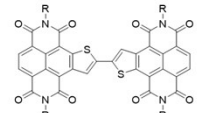
Calculations of intermolecular transfer integrals of LUMOs were performed with the PBE0 functional and Slater-type double- $\zeta$  plus polarization (DZP) basis sets using the ADF (Amsterdam Density Functional) package.<sup>4</sup>

## 2. Comparison of phase transition temperature and solubility between linear and helically-twisted polycyclics



**Figure S1.** Illustration images of molecular rotation in the solid state of linear-acenes (a) and helically-twisted molecules (b) with solubilizing groups.

**Table S1.** Solubility and phase transition temperature of two-NDI incorporated polycyclic molecules with twisted structure and planar structure.

Compound <sup>[a]</sup>	Solubility in CHCl <sub>3</sub> / g L <sup>-1</sup> [b]	Phase transition temp. from solid to liquid crystal / °C
	5.6	>300
	0.052	174

[a] R = C<sub>8</sub>H<sub>17</sub>. [b] room temperature.

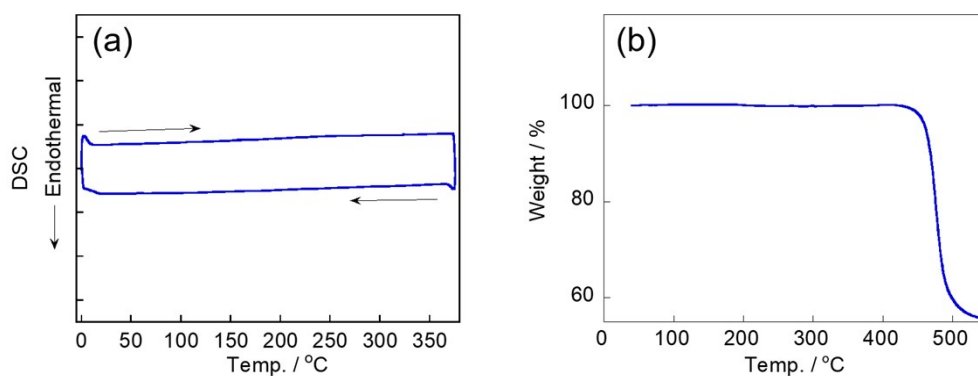


**Figure S2.** DSC (a) and TG (b) curves of compound **1** (10°C min<sup>-1</sup>, N<sub>2</sub>).

### 3. DFT calculation results

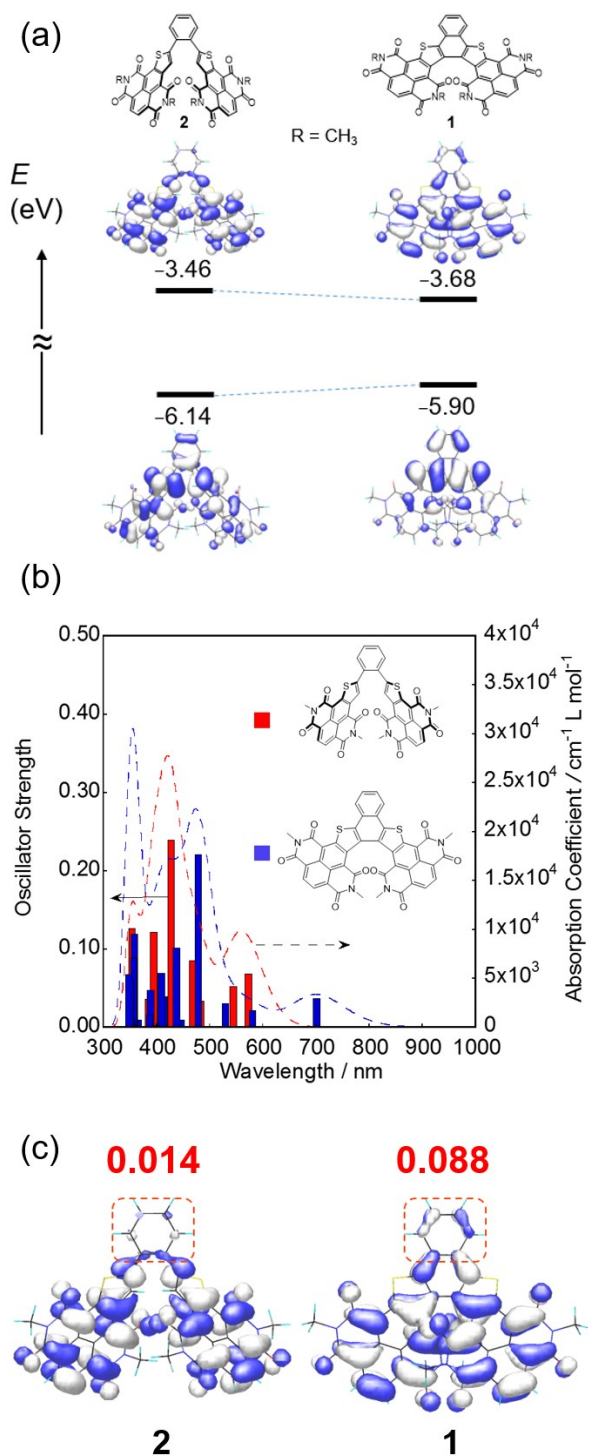


**Figure S3.** DFT-optimized molecular structures and molecular orbitals (a), simulated absorption spectra (b), and LUMO coefficients at the central benzene moieties (c) of **1** and **2** (B3LYP/6-31G\*). The model compounds have methyl groups at their imide moieties to simplify the calculations.

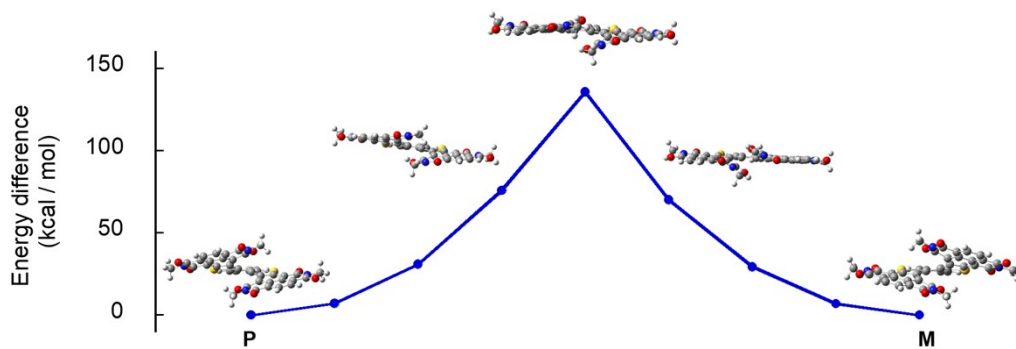


**Figure S4.** Calculated isomerization energy from P- to M-isomer of **1** (B3LYP/6-31G\*)

#### 4. Dihedral angles of the inner C-C bonds and bonds of NDI moiety of **1**

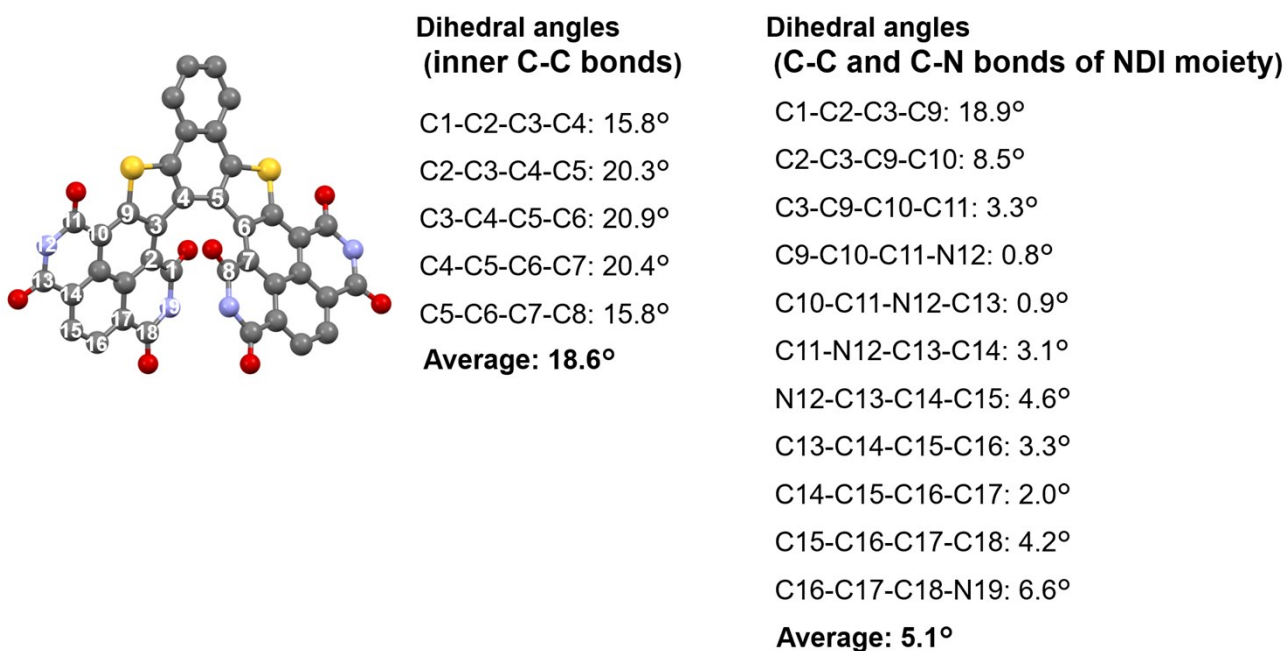


**Figure S5.** Dihedral angles of the inner C-C bonds and bonds of NDI moiety of **1** from the structure measured by single-crystal X-ray analysis.

## 5. Single-crystal X-Ray measurement

Single crystals of **1** for X-ray structural analysis were obtained by recrystallization from nitrobenzene. The single-crystal X-ray diffraction analyses of **1** was carried out at the BL40XU and BL02B1 beam lines of the SPring-8 synchrotron. All frame images (Dectris) were converted to the SFRM format using *Henkankun-R*.<sup>5</sup> Data reduction was performed using Bruker SAINT. Structures were solved by direct methods (*SHELXT-2014*) and refined against *F*<sup>2</sup> by weighted full-matrix least-squares (*SHELXL-2014*).<sup>6</sup> Crystallographic data of **1** was deposited at the CCDC under reference numbers CCDC-2002621.

Crystallographic data for **1**: C<sub>70</sub>H<sub>70</sub>N<sub>4</sub>O<sub>8</sub>S<sub>2</sub> (1159.42), dark-green platelet needle, 0.40 × 0.10 × 0.05 mm<sup>3</sup>, monoclinic, space group, C2/c (#15), a = 33.803(7), b = 13.242(3), c = 13.405(3) Å, α = 90°, β = 108.746 (3)°, γ = 90°, V = 5682.4(19) Å<sup>3</sup>, Z = 4, R(F) = 0.733 for 6510 observed reflections (I > 2σ(I)) and 515 variable parameters, wR(F<sub>2</sub>) = 0.2709 for all data.

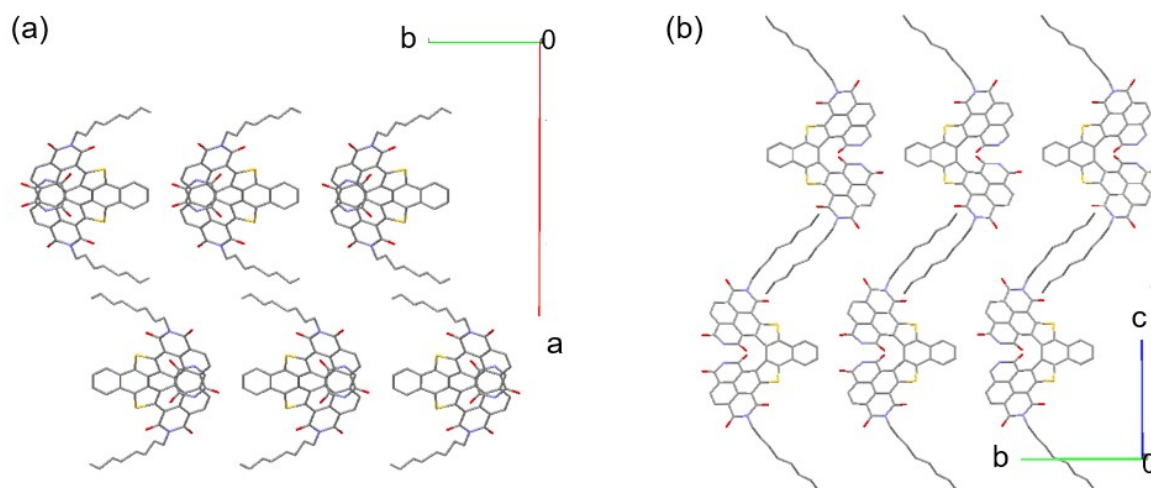


**Fig. S6.** Molecular arrangement of **1** in single crystal viewed in the vertical direction of the *c*-axis (a) and the *a*-axis (b).

6. Changes of XRD patterns and AFM images of thin film of **1** upon thermal annealing

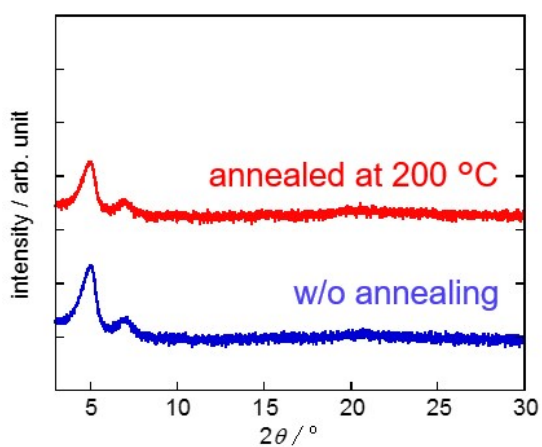


**Fig. S7.** Changes of XRD patterns of thin film of **1** with thermal annealing (1 h).

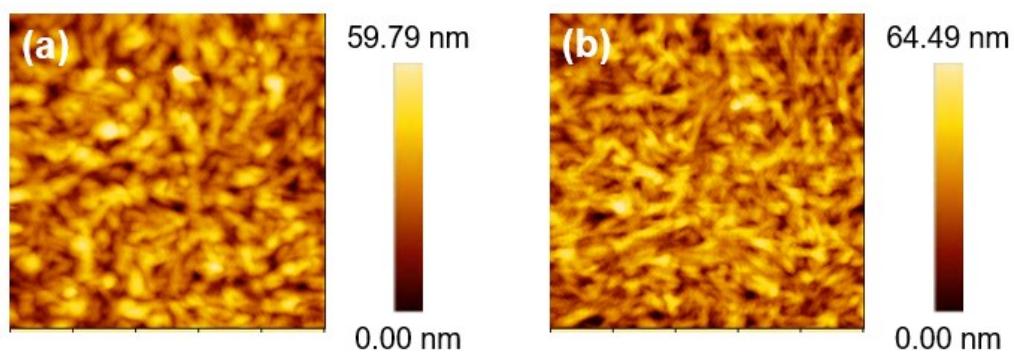


**Fig. S8.** AFM images of thin film of **1** without thermal annealing (a) and with annealing at 200 °C (1 h) (b).

## 7. Fabrication methods and properties of OTFT devices

**1**-based OTFT devices were fabricated in a top-contact/bottom-gate configuration on a heavily doped  $n^+$ -Si (100) wafer with a 200 nm thermally grown  $\text{SiO}_2$  (capacitance:  $C_i = 17.3 \text{ nF cm}^{-2}$ ). The substrate was carefully treated with octadecyltrichlorosilane (ODTS) as reported previously.<sup>7</sup> The thin films of **1** were fabricated by the spin-coating method (7500 rpm, 30 sec) using chloroform solution ( $4 \text{ g L}^{-1}$ ), and then, the films were annealed at  $150^\circ\text{C}$  (10 min) for drying under nitrogen conditions. On the top of the organic thin film, gold films (80 nm) as drain and source electrodes were deposited through a shadow mask. For a typical device, the drain-source channel length ( $L$ ) and width ( $W$ ) are  $40 \text{ }\mu\text{m}$  and  $1.5 \text{ mm}$ , respectively. The device characteristics were measured at room temperature under ambient conditions (humidity:  $<20\%$ ). Field-effect mobility ( $\mu$ ) was calculated in the saturation regime ( $V_g = 40\text{-}60 \text{ V}$ ) using the following equation,

$$I_d = C_i \mu (W/2L) (V_g - V_{th})^2$$

where  $C_i$  is the capacitance of the  $\text{SiO}_2$  insulator, and  $V_g$  and  $V_{th}$  are the gate and threshold voltages, respectively. Reliability factor ( $r$ ) of the devices is calculated as reported by Choi *et al.*<sup>8</sup> The calculated  $r$  value is  $0.30 (\pm 0.07)$ .

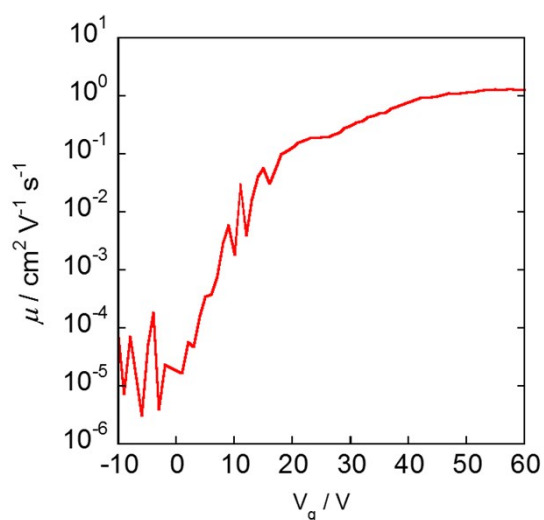
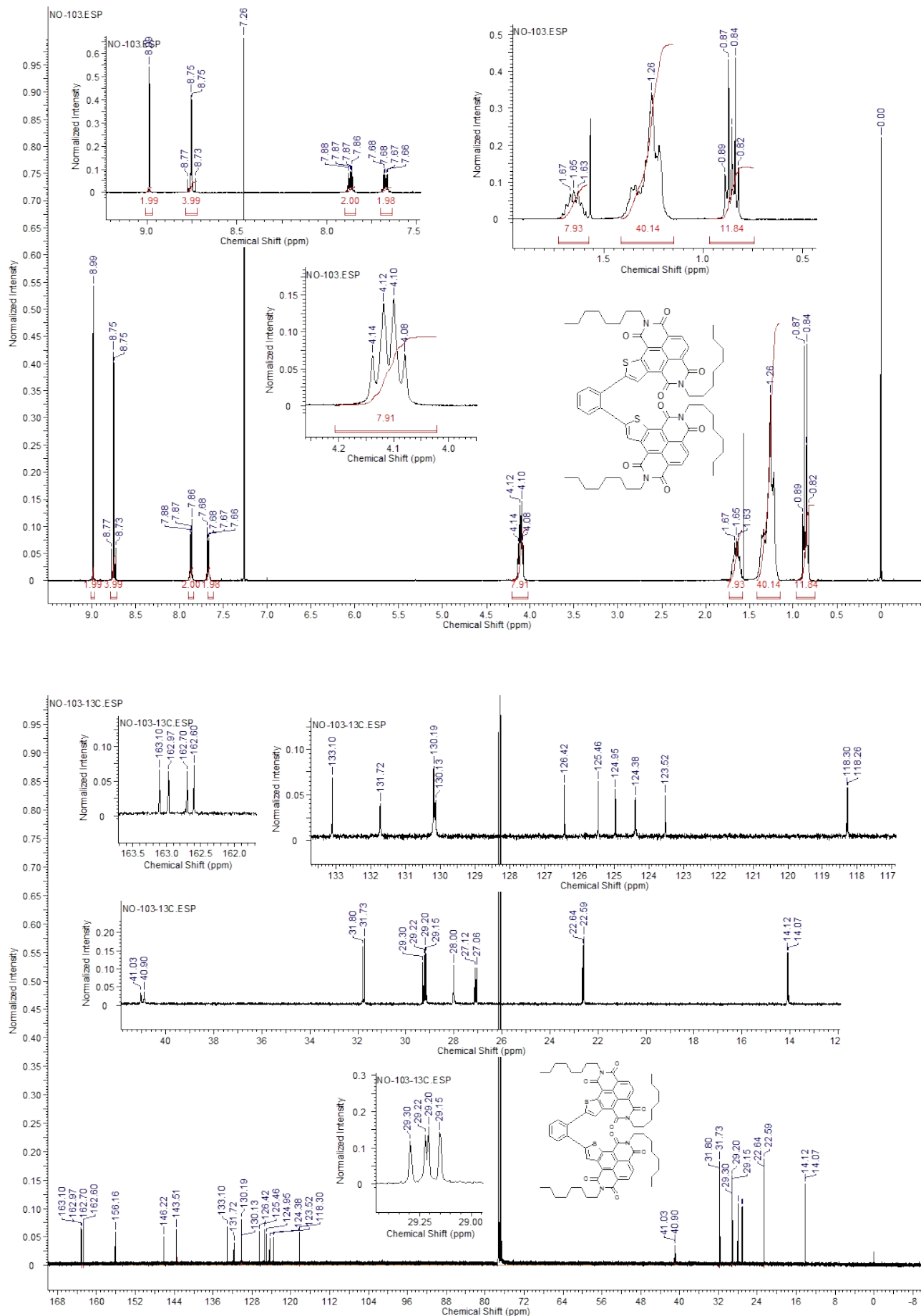


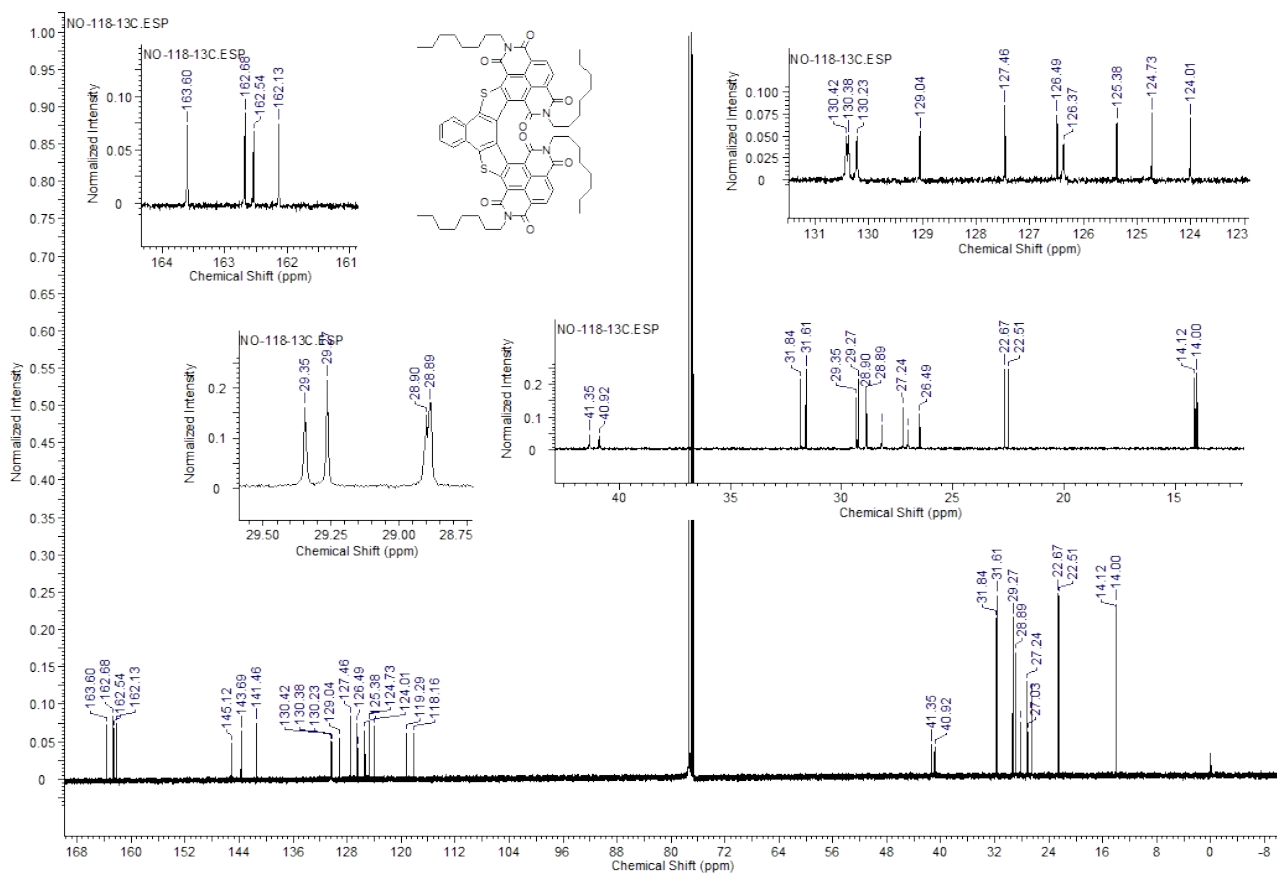
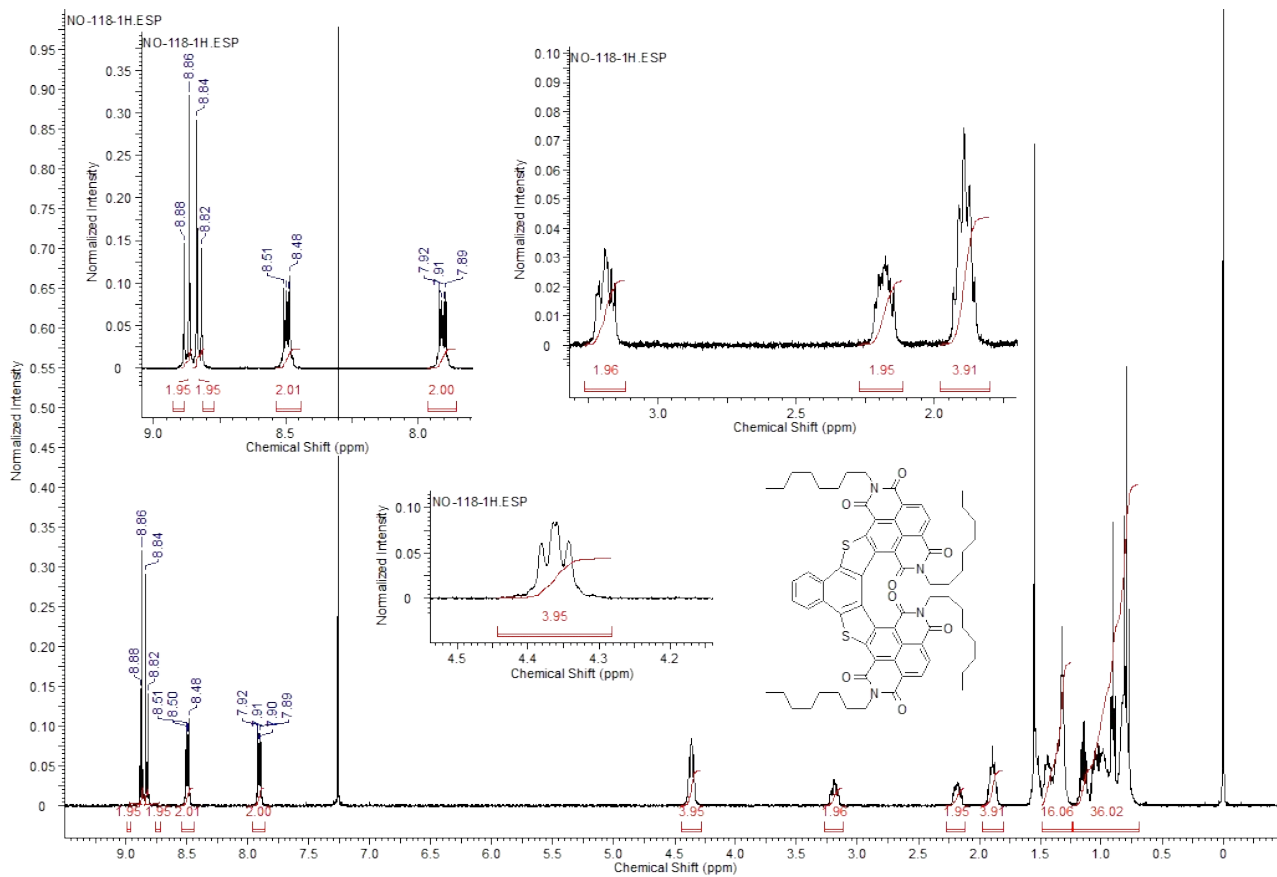
**Figure S9.** Gate-voltage dependence of mobility.

**Table S2.** TFT performances of thermally annealed devices.

Anneal / °C	$\mu$ / $\text{cm}^2\text{V}^{-1}\text{s}^{-1}$	$I_{on}/I_{off}$	$V_{th}$ / V
w/o	1.20±0.22	~2.4×10 <sup>8</sup>	29.4±5.9
100	1.18±0.14	~3.4×10 <sup>8</sup>	32.4±1.6
150	1.06±0.15	~3.3×10 <sup>8</sup>	33.7±1.2
200	1.22±0.14	~2.2×10 <sup>8</sup>	31.2±2.6

## 8. NMR charts





## 9. References

- 
- <sup>1</sup> R. Matsidik, K. Takimiya, *Chem. Asian, J.* **2019**, *14*, 1651–1656
- <sup>2</sup> Gaussian 09, Revision D.01, Frisch, M. J.; Trucks, G. W.; Schlegel, H. B.; Scuseria, G. E.; Robb, M. A.; Cheeseman, J. R.; Scalmani, G.; Barone, V.; Mennucci, B.; Petersson, G. A.; Nakatsuji, H.; Caricato, M.; Li, X.; Hratchian, H. P.; Izmaylov, A. F.; Bloino, J.; Zheng, G.; Sonnenberg, J. L.; Hada, M.; Ehara, M.; Toyota, K.; Fukuda, R.; Hasegawa, J.; Ishida, M.; Nakajima, T.; Honda, Y.; Kitao, O.; Nakai, H.; Vreven, T.; Montgomery, J. A., Jr.; Peralta, J. E.; Ogliaro, F.; Bearpark, M.; Heyd, J. J.; Brothers, E.; Kudin, K. N.; Staroverov, V. N.; Kobayashi, R.; Normand, J.; Raghavachari, K.; Rendell, A.; Burant, J. C.; Iyengar, S. S.; Tomasi, J.; Cossi, M.; Rega, N.; Millam, J. M.; Klene, M.; Knox, J. E.; Cross, J. B.; Bakken, V.; Adamo, C.; Jaramillo, J.; Gomperts, R.; Stratmann, R. E.; Yazyev, O.; Austin, A. J.; Cammi, R.; Pomelli, C.; Ochterski, J. W.; Martin, R. L.; Morokuma, K.; Zakrzewski, V. G.; Voth, G. A.; Salvador, P.; Dannenberg, J. J.; Dapprich, S.; Daniels, A. D.; Farkas, Ö.; Foresman, J. B.; Ortiz, J. V.; Cioslowski, J.; Fox, D. J. Gaussian, Inc., Wallingford CT, **2009**.
- <sup>3</sup> Reaction Plus Pro; HPC systems Inc.; <https://www.hpc.co.jp/eng/>
- <sup>4</sup> ADF: powerful DFT code for modeling molecules; Scientific Computing and Modeling: Amsterdam; <http://www.scm.com/ADF/>
- <sup>5</sup> *Henkankun-R* is software for the conversion from Dectris-PILATUS and EIGER frames to the SFRM format, cf. S. Shikama, R. Nishino, M. Minoura, November, 2018, available at SPring-8.
- <sup>6</sup> Sheldrick, G., Crystal structure refinement with SHLXL. *Acta Cryst. C* **2015**, *71*, 3–8.
- <sup>7</sup> K. Takimiya, H. Ebata, K. Sakamoto, T. Izawa, T. Otsubo, Y. Kunugi, *J. Am. Chem. Soc.* **2006**, *128*, 12604–12605.
- <sup>8</sup> H. H. Choi, K. Cho, C. D. Frisbie, H. Sirringhaus, V. Podzorov, *Nat. Mater.* **2018**, *17*, 2–7.